

Studies of Nonlinear Two Fluid Tearing Modes in Cylindrical Reversed Field Pinches

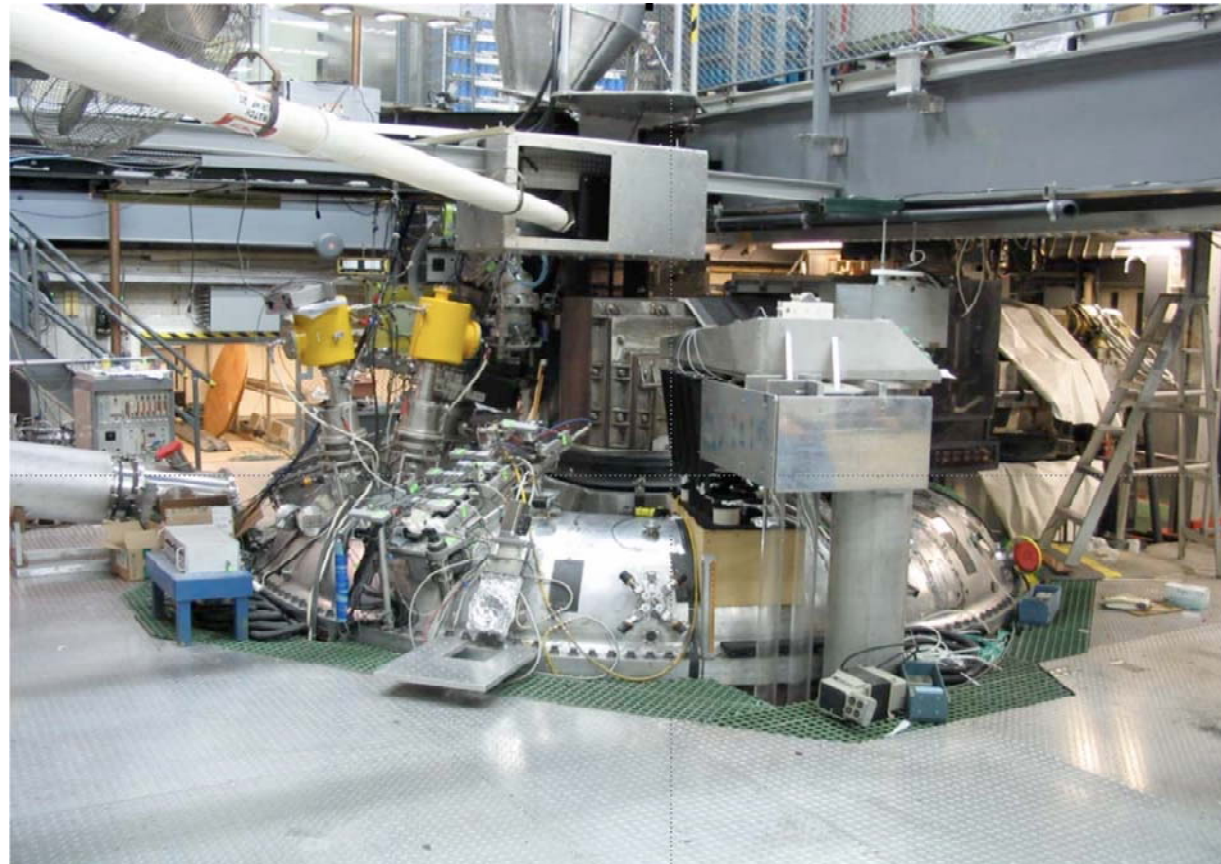
V. V. Mirnov, J. R. King and C. R. Sovinec

University of Wisconsin-Madison and Center for Magnetic Self - Organization in Laboratory and Astrophysical Plasmas



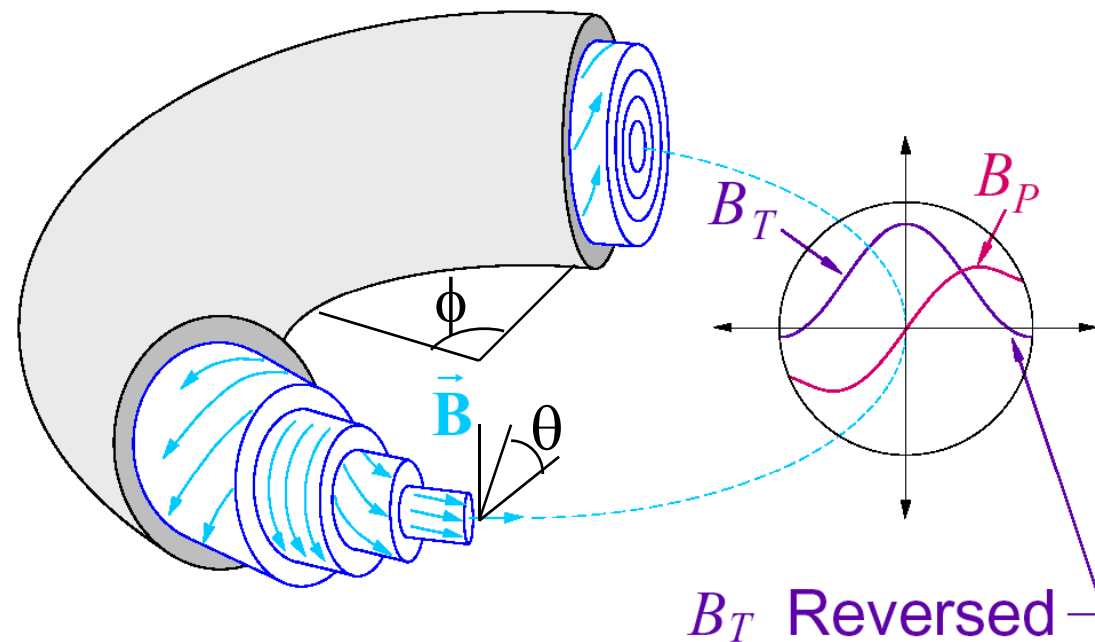
2008 US-Japan Workshop "Progress of Multi-Scale Simulation Models", Nov. 21-22, Dallas, TX

The Madison Symmetric Torus RFP experiment



$R = 1.5 \text{ m}$, $a = 0.5 \text{ m}$, $I \sim 0.5 \text{ MA}$, $T \leq 1 \text{ keV}$, $n \leq 10^{13} \text{ cm}^{-3}$

Magnetic configuration of Reversed Field Pinch



- Toroidal field B_T is ~ 5 times smaller than same-current tokamak
- Equilibrium substantially determined by self-generated plasma currents

RFP equilibrium - resonant unstable modes exist

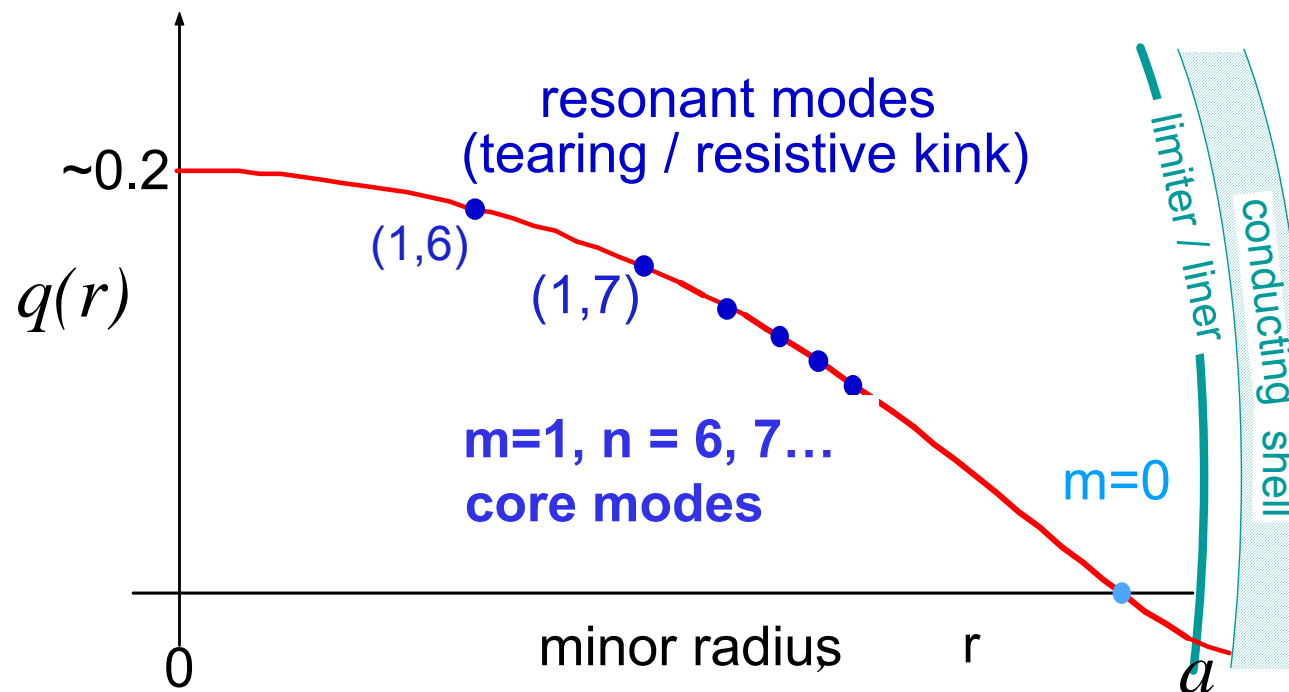


$$\tilde{\mathbf{B}} = \sum_{n,m} \tilde{\mathbf{B}}_{mn}(r) \exp(im\theta + inz/R)$$

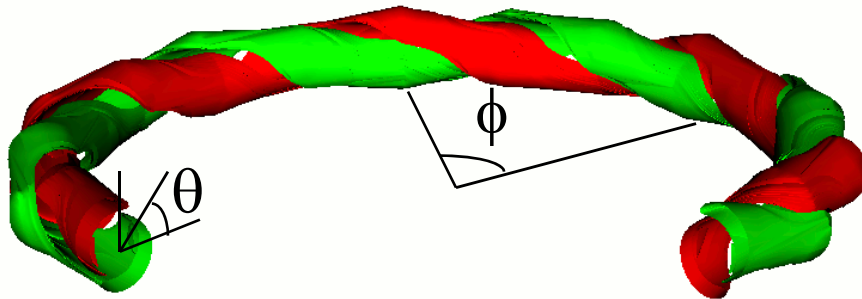
➤ $\mathbf{k} \cdot \mathbf{B} = m B_p / r - n B_T / R = 0 \rightarrow m/n = q(r) = r B_T / R B_p$

➤ Stability depends on $\lambda(r) = J_{\parallel} / B$

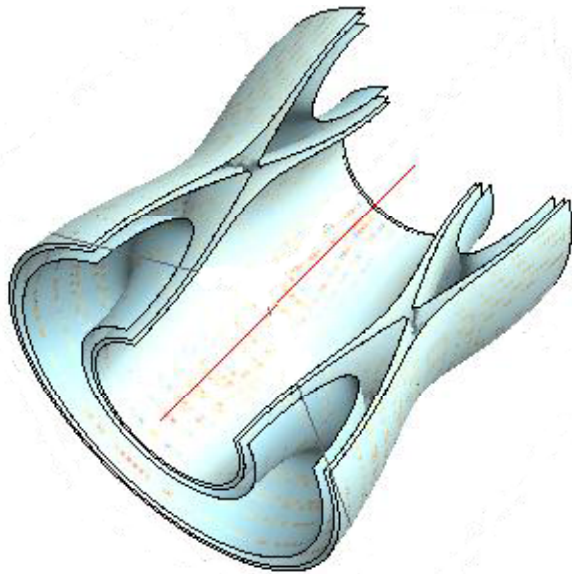
MST Reversed Field Pinch



3D structure of core and edge modes



3D magnetic perturbations
($m=1, n=6$ core mode)

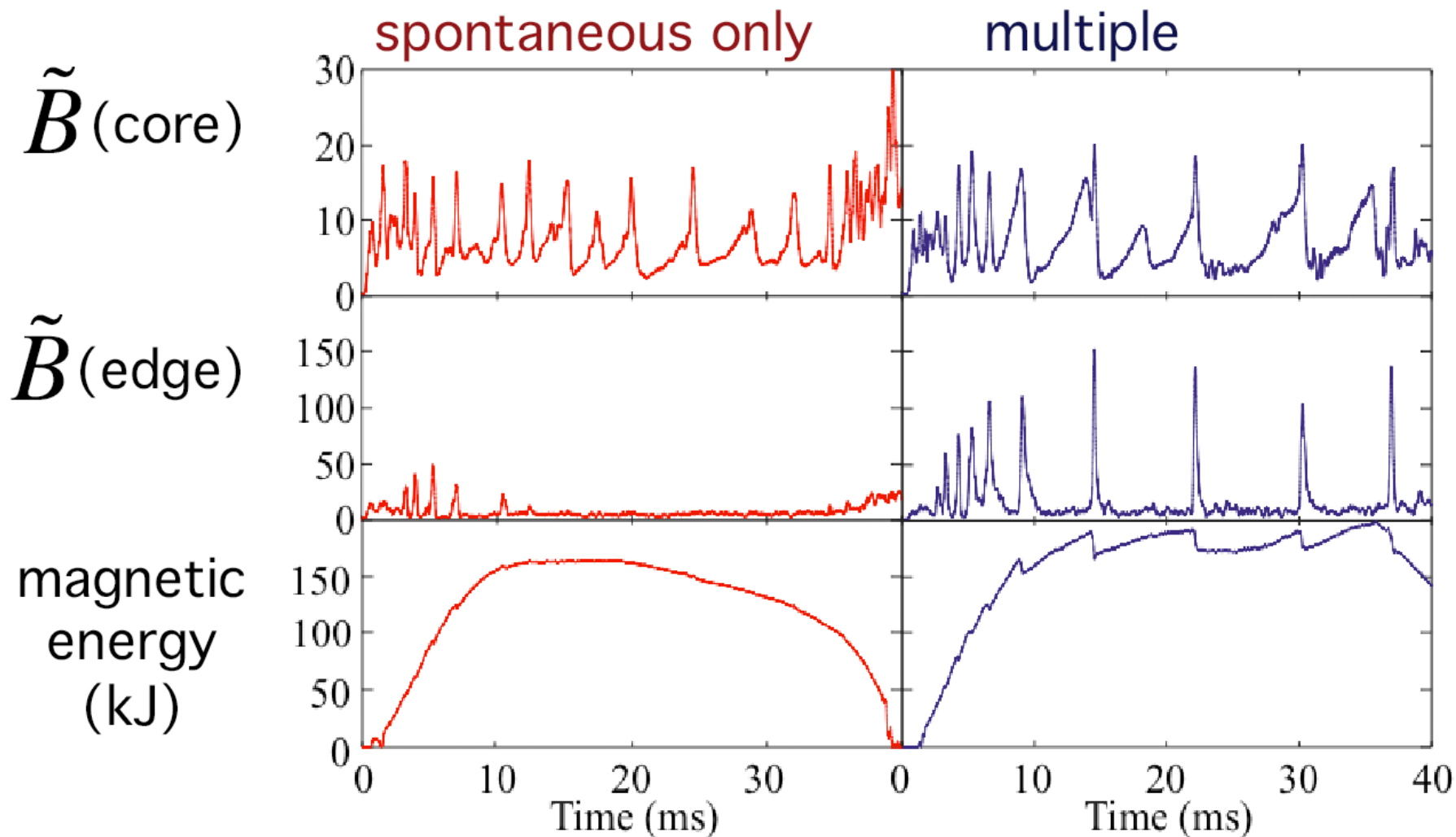


magnetic surfaces for
 $m=0, n=1$ edge mode

two unstable core modes are
nonlinearly coupled to the edge mode

$$\mathbf{k}_{1,7} + \mathbf{k}_{-1,-6} = \mathbf{k}_{0,1}$$

Large magnetic energy only occurs with both core *and* edge reconnection



Multi-scales of two fluid MHD: key findings



resistive tearing layer

$$w_T \sim a/S^{2/5}$$

ion-sound gyroradius

$$\rho_s \sim (1/\omega_{ci}) [(T_e + T_i) / m]^{1/2}$$

minor radius

a

Linear tearing mode

- **Two-fluid physics + cylindrical field line curvature**



complex growth rate (mode rotation) without $\omega_{*i,e}$ effects

Nonlinear NIMROD simulations

- **Small modification of the mean current is enough for nonlinear mode saturation**
- **Hall dynamo is broadened in cylindrical geometry contrary to the fine structure along the separatrix observed in 2D slab simulations**

Cylindrical RFP configuration brings new effects into play



- Radial component of the induction equation

$$\frac{\partial B_r}{\partial t} - \frac{\eta c^2}{4\pi} \nabla^2 \mathbf{B}|_r = ik_{\parallel} B v_r + \frac{ik_{\parallel}}{ne} (\mathbf{j}^{(1)} \times \mathbf{B} + \mathbf{j} \times \mathbf{B}^{(1)})|_{\perp} = -\frac{ck_{\parallel} k_{\perp}}{ne} p^{(1)}$$

- Parallel component with curvature and current gradient effects

$$\frac{\partial B_{\parallel}}{\partial t} + \boxed{B \nabla \cdot \mathbf{v}_{\perp}} - v_r \frac{2B_{\theta}^2}{rB} - \frac{\eta c^2}{4\pi} \nabla^2 \mathbf{B}|_{\parallel} = -\frac{1}{ne} \mathbf{b} \cdot \nabla \times (\mathbf{j}^{(1)} \times \mathbf{B} + \mathbf{j} \times \mathbf{B}^{(1)})$$

$ik_{\perp} p^{(1)} (d \ln B^2 / dr)$
 $BB_r d/dr (j/B)$

- Force balance in cross-field $\mathbf{b} \times \mathbf{e}_r$ direction

$$p^{(1)} = -\frac{k_0^2}{k_{\perp}^2} \frac{BB_{\parallel}}{4\pi} + \frac{j}{ik_{\perp} c} B_r + \frac{ik_{\parallel} B}{4\pi k_{\perp}^2} \frac{\partial}{\partial r} (r B_r)$$

- Two fluid tearing instability is driven mainly by the electrons.
- Ion motion enters the equations through the plasma compressibility.
- Equilibrium diamagnetic flows are ignored (force free equilibrium).

Tearing equations are simplified on short scales



- Coupled equations for two fluid cylindrical tearing mode

$$\left[1 + B^2 \left(\frac{1}{\beta} + \frac{k_{\parallel}^2}{\gamma^2} \right) + \frac{2id_i k_0 B_{\theta}^2}{\gamma r B} \right] \tilde{B}_{\parallel} - \delta^2 \frac{d^2 \tilde{B}_{\parallel}}{dr^2} = \frac{d_i B}{\gamma} \left(\frac{k_{\parallel}}{k_0} \frac{\partial^2 B_r}{\partial r^2} - \frac{d\lambda}{dr} B_r \right), \quad \lambda = \frac{4\pi j a}{c B_0 B}$$

$$B_r - \delta^2 \frac{d^2 B_r}{dr^2} = \frac{d_i k_{\parallel} k_0 B}{\gamma} \tilde{B}_{\parallel}, \quad \beta = \frac{4\pi p^{(0)} \Gamma}{B_0^2}, \quad \Gamma = 5/3, \quad \gamma \rightarrow \gamma \tau_A, \quad \delta^2 = \frac{1}{\gamma S}$$

- Renormalized function B_{\parallel}

$$B_{\parallel} = \tilde{B}_{\parallel} - \frac{i\lambda}{k_0} B_r$$

- Quasi-linear approach to mean field characteristics

$$(1/en^{(0)}c) \langle \mathbf{j}^{(1)} \times \mathbf{B}^{(1)} \rangle_{\parallel} - (1/c) \langle \mathbf{v}^{(1)} \times \mathbf{B}^{(1)} \rangle_{\parallel} = \langle \mathbf{E} \rangle_{\parallel} - \eta \langle \mathbf{j} \rangle_{\parallel},$$

Hall dynamo

MHD dynamo

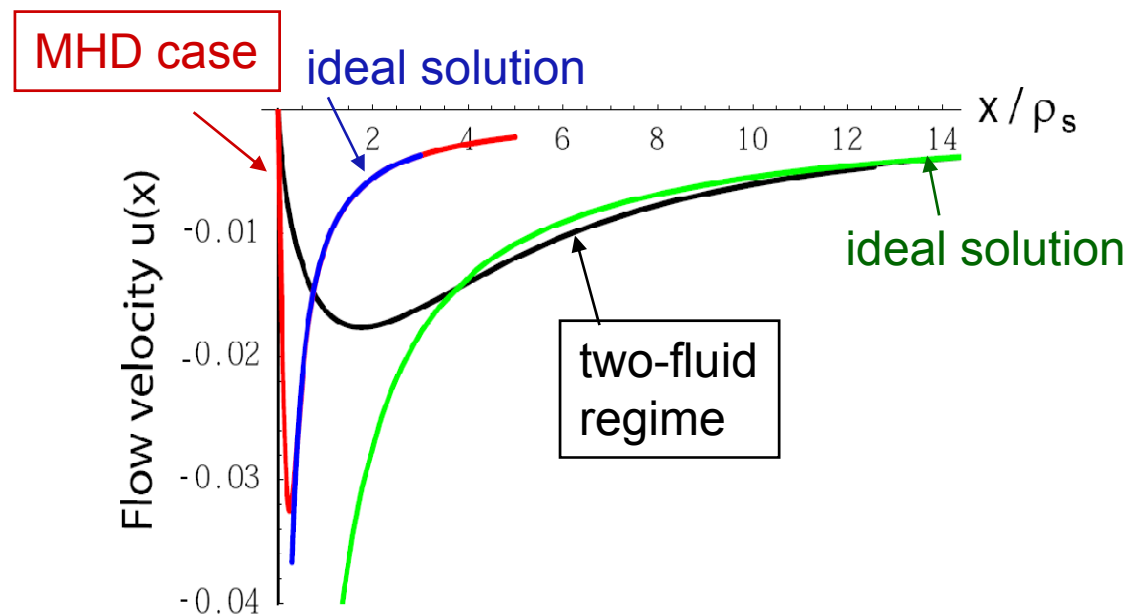
- Cross-phase between B_r and B_{\parallel} determines the Hall dynamo

$$\epsilon_{\parallel}^{(H)} = \epsilon_0 d_i \langle \mathbf{b}^{(0)} [\text{Re } \mathbf{j}^{(1)} \times \text{Re } \mathbf{B}^{(1)}] \rangle = \frac{\epsilon_0 d_i}{2r} \text{Re} \frac{\partial}{\partial r} (r B_r B_{\parallel}^*), \quad \epsilon_0 = B_0 \frac{v_A}{c}$$

Plasma flow velocities are reduced and broaden to large ρ_s scale



- Flow profiles in two limiting cases:
 - $\rho_s S^{2/5} = 0.1$ (MHD)
 - $\rho_s S^{2/5} = 10$ (two-fluid)



- Amplitudes of the flow velocities in 2F and 1F cases

$$u_{max}^{(2F)} \propto \frac{1}{\rho_s^{1/3} S^{1/3}}, \quad u_{max}^{(MHD)} \propto \frac{1}{S^{1/5}} \rightarrow \frac{u_{max}^{(MHD)}}{u_{max}^{(2F)}} \simeq (\rho_s S^{2/5})^{1/3}$$

NIMROD is an initial value solver that capable of modeling the two fluid tearing instability



$$\frac{\partial \mathbf{B}}{\partial t} = -\nabla \times \left(\eta \mathbf{J} - \mathbf{V} \times \mathbf{B} + \frac{1}{ne} \mathbf{J} \times \mathbf{B} - \frac{1}{ne} \nabla p_e \right) \quad \text{Faraday's / Ohm's law}$$

$$\mu_0 \mathbf{J} = \nabla \times \mathbf{B} \quad \text{Ampere's law}$$

$$\nabla \cdot \mathbf{B} = 0 \quad \text{divergence constraint}$$

$$\rho \left(\frac{\partial \mathbf{V}}{\partial t} + \mathbf{V} \cdot \nabla \mathbf{V} \right) = \mathbf{J} \times \mathbf{B} - \nabla p + \nabla \cdot \nu \rho \mathbf{W}$$

$$\left(\mathbf{W} \equiv \nabla \mathbf{V} + \nabla \mathbf{V}^T - \frac{2}{3} \mathbf{I} \nabla \cdot \mathbf{V} \right) \quad \text{flow evolution}$$

$$\frac{\partial n}{\partial t} + \nabla \cdot (n \mathbf{V}) = \nabla \cdot D \nabla n \quad \text{particle continuity with artificial diffusivity}$$

$$\frac{n}{\gamma - 1} \left(\frac{\partial T_\alpha}{\partial t} + \mathbf{V}_\alpha \cdot \nabla T_\alpha \right) = -p_\alpha \nabla \cdot \mathbf{V}_\alpha + \nabla \cdot n \chi \nabla T_\alpha \quad \text{temperature evolution}$$

- We set D , χ , and $\nu \ll \eta / \mu_0$.

Equilibrium magnetic configuration of the paramagnetic pinch



- Force-free equilibrium

$$\mathbf{j} = \lambda(r)\mathbf{B}$$

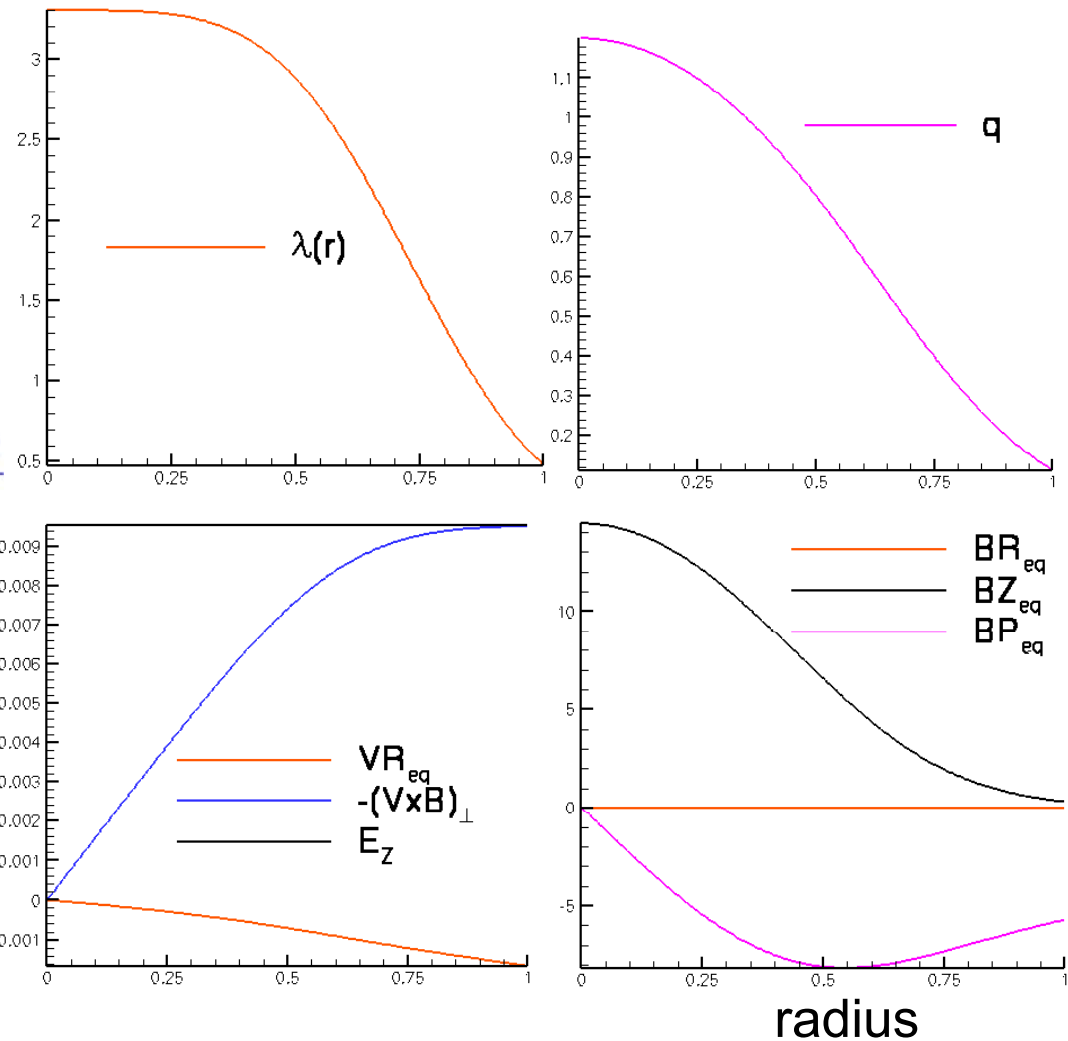
- External electric field \mathbf{E}_z determines λ

$$\mathbf{E} + \frac{1}{c}\mathbf{v} \times \mathbf{B} = \eta\mathbf{j} \rightarrow \lambda = \frac{E_z B_z(r)}{\eta B^2(r)}$$

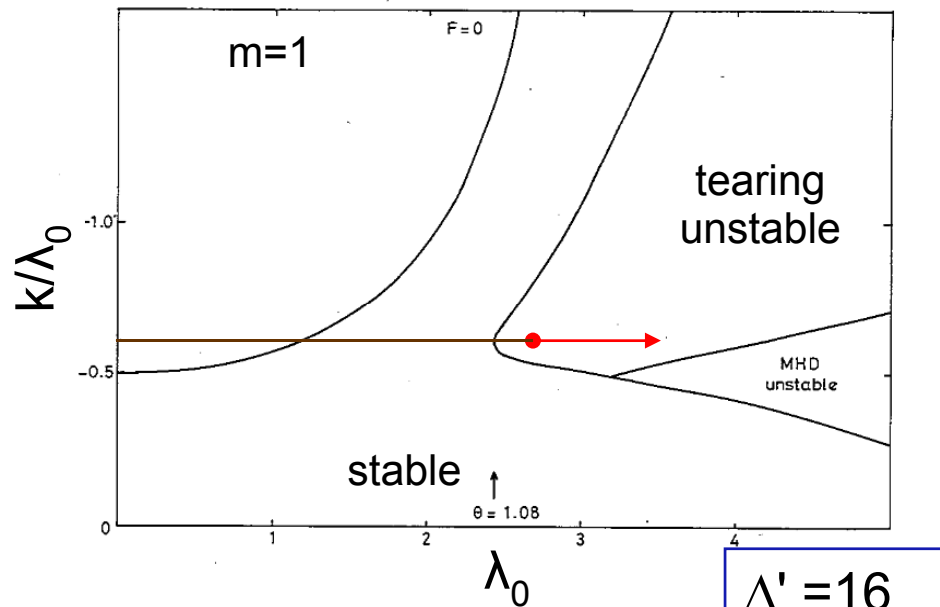
- Ampere's law \rightarrow magnetic configuration is determined by one dimensionless parameter λ_0

$$\nabla \times \bar{\mathbf{B}} = \lambda_0 \frac{\bar{\mathbf{B}} \bar{B}_z}{\bar{B}^2}, \quad \lambda_0 = \frac{4\pi E_z a}{\eta c B(0)}, \quad \bar{\mathbf{B}} = \mathbf{B}/B(0), \quad r \rightarrow r/a$$

(2) $\lambda_0 = 3.3$, $S = 5 \times 10^3$



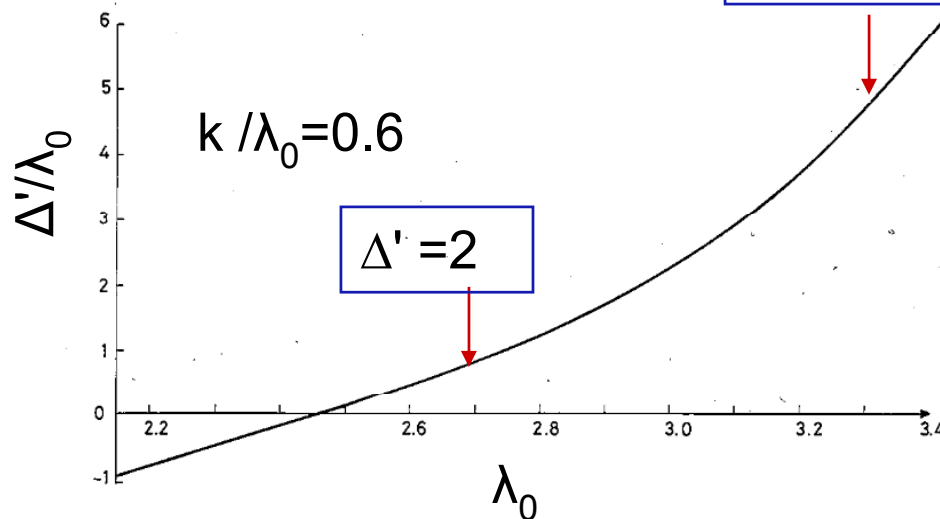
Robinson's study of paramagnetic equilibrium provides a map of the linear stability



The mode is growing if stability factor $\Delta' > 0$

$$\Delta' = \frac{1}{B_r} \left[\frac{\partial B_r}{\partial r} (+0) - \frac{\partial B_r}{\partial r} (-0) \right]$$

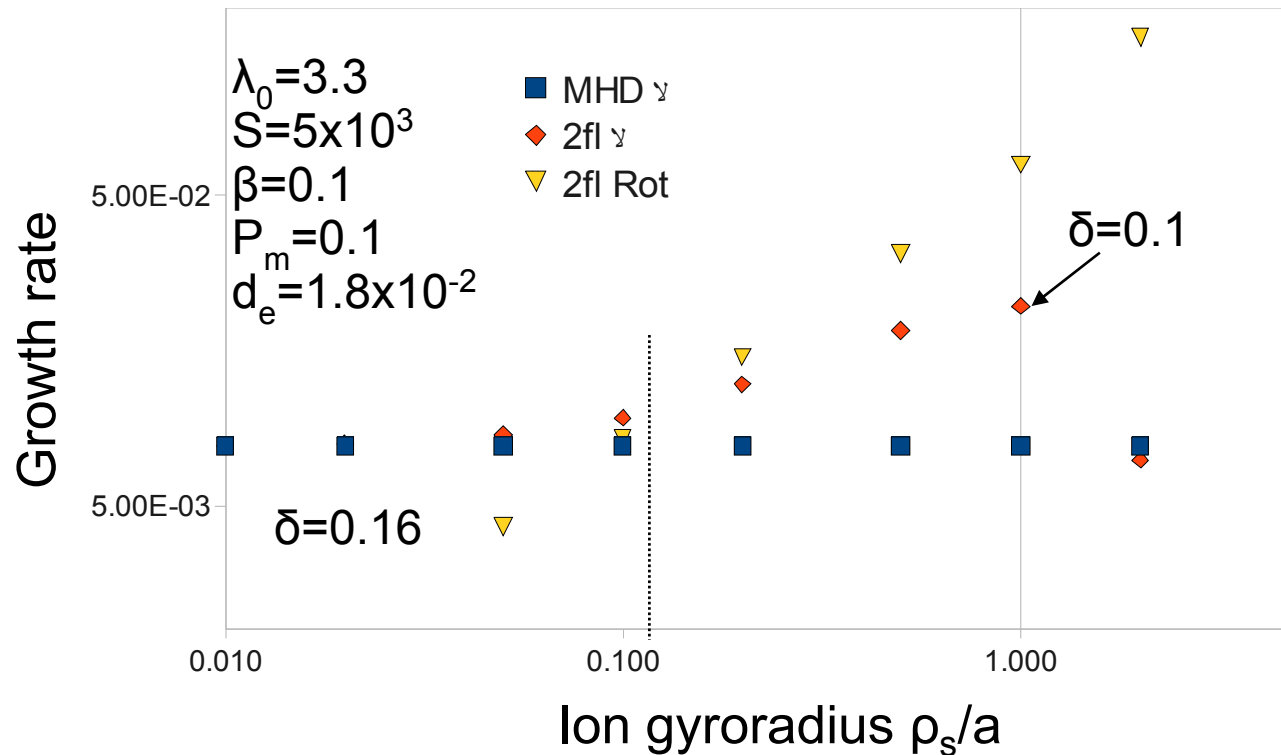
$k / \lambda_0 = 0.6$ with $\lambda_0 = 2.7$ are chosen initially to provide a mode close to marginal stability with $\Delta' = 2$.



more unstable modes with $\Delta' = 16$ are studied at $\lambda_0 = 3.3$ (k/λ_0 remains constant to keep q_0 constant).

D.C. Robinson, Nucl. Fusion (1978)

The growth rate and mode rotation scales with ρ_s



Electron skin-depth

$$\delta^2 = d_e^2 + \frac{1}{\gamma \tau_a S}$$

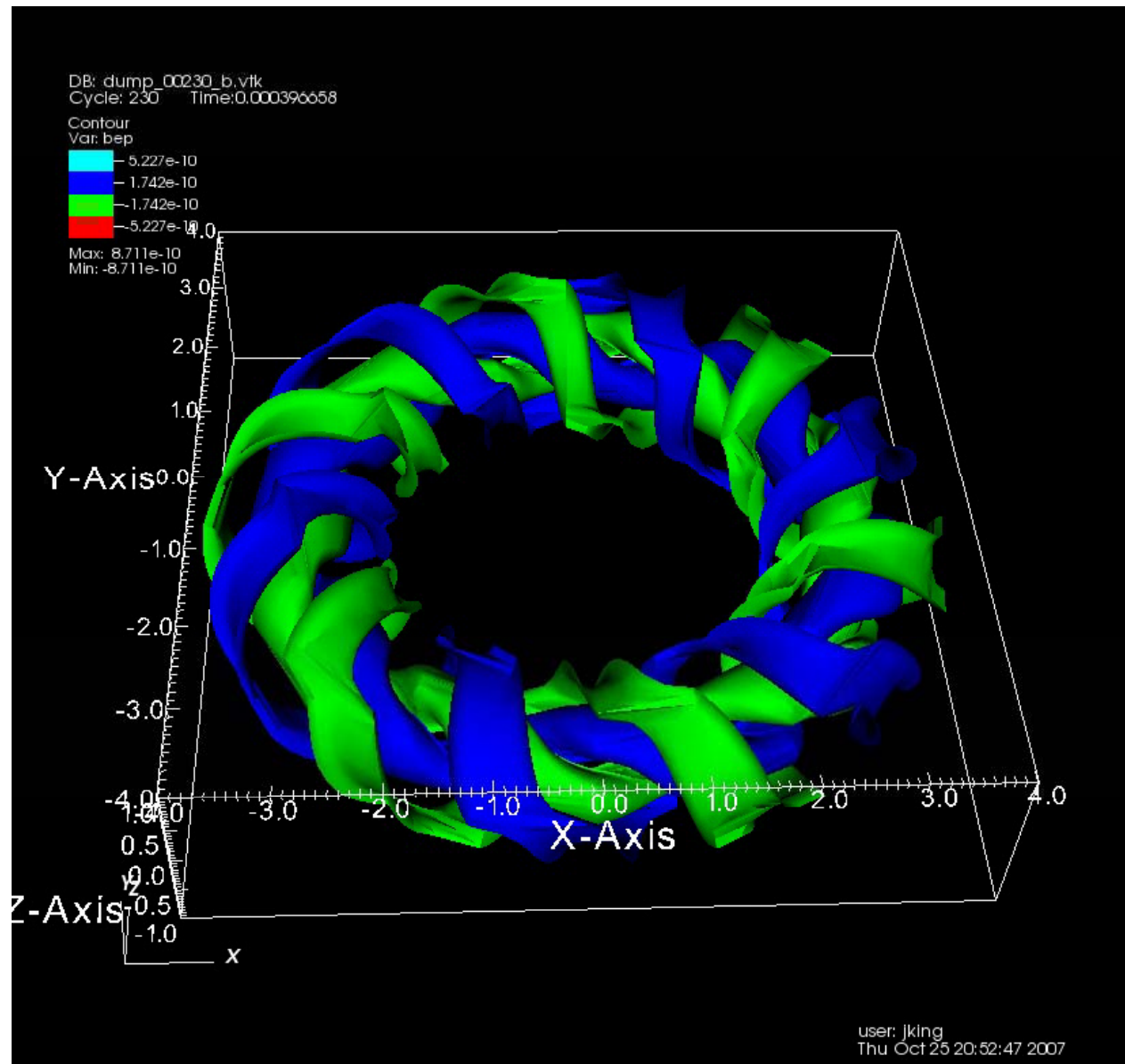
collisionless part d_e
is small compared
to the resistive term

Some examples
of plasma
parameters:

$B_0=0.4$ T
 $n=1 \times 10^{19}$ m⁻³
 $\beta=0.1$
 $a=0.51$ m
 $\rho_s/a=5.8 \times 10^{-2}$

$B_0=0.2$ T
 $n=1 \times 10^{18}$ m⁻³
 $\beta=0.1$
 $a=0.51$ m
 $\rho_s/a=1.8 \times 10^{-1}$

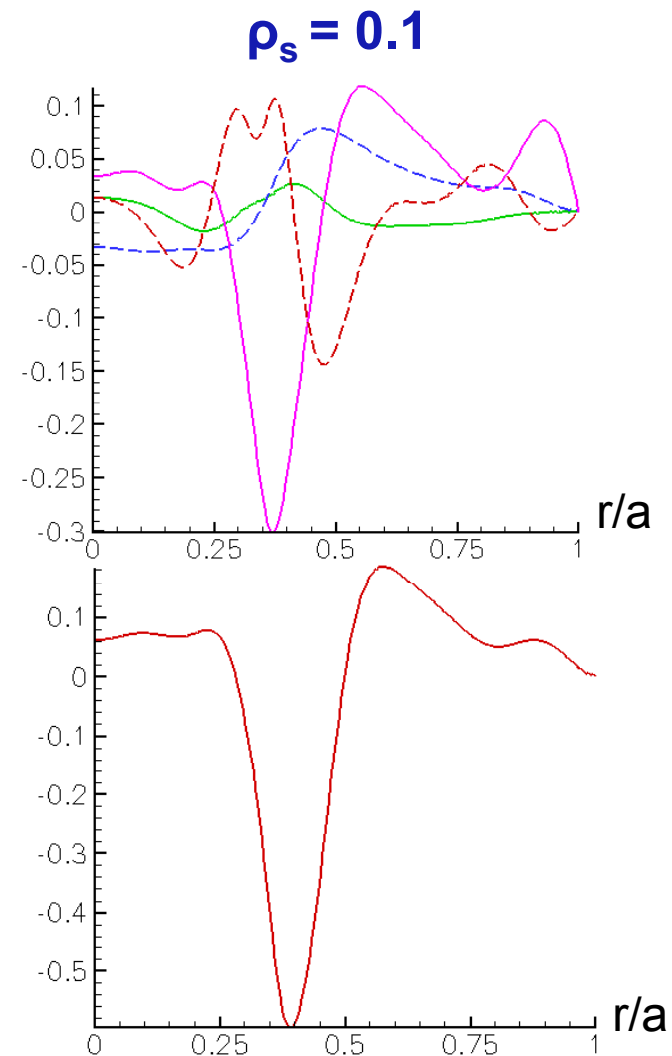
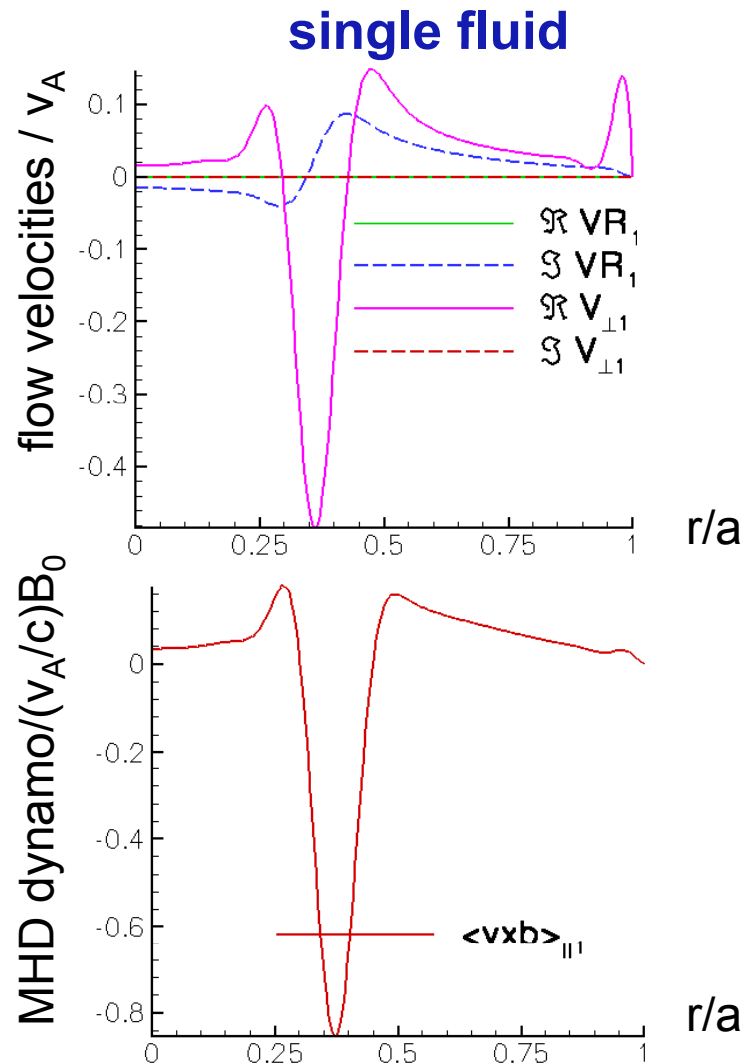
2F dynamics and curvature effects result in mode rotation without diamagnetic flows



The quasilinear MHD dynamo is broadened at large ρ_s



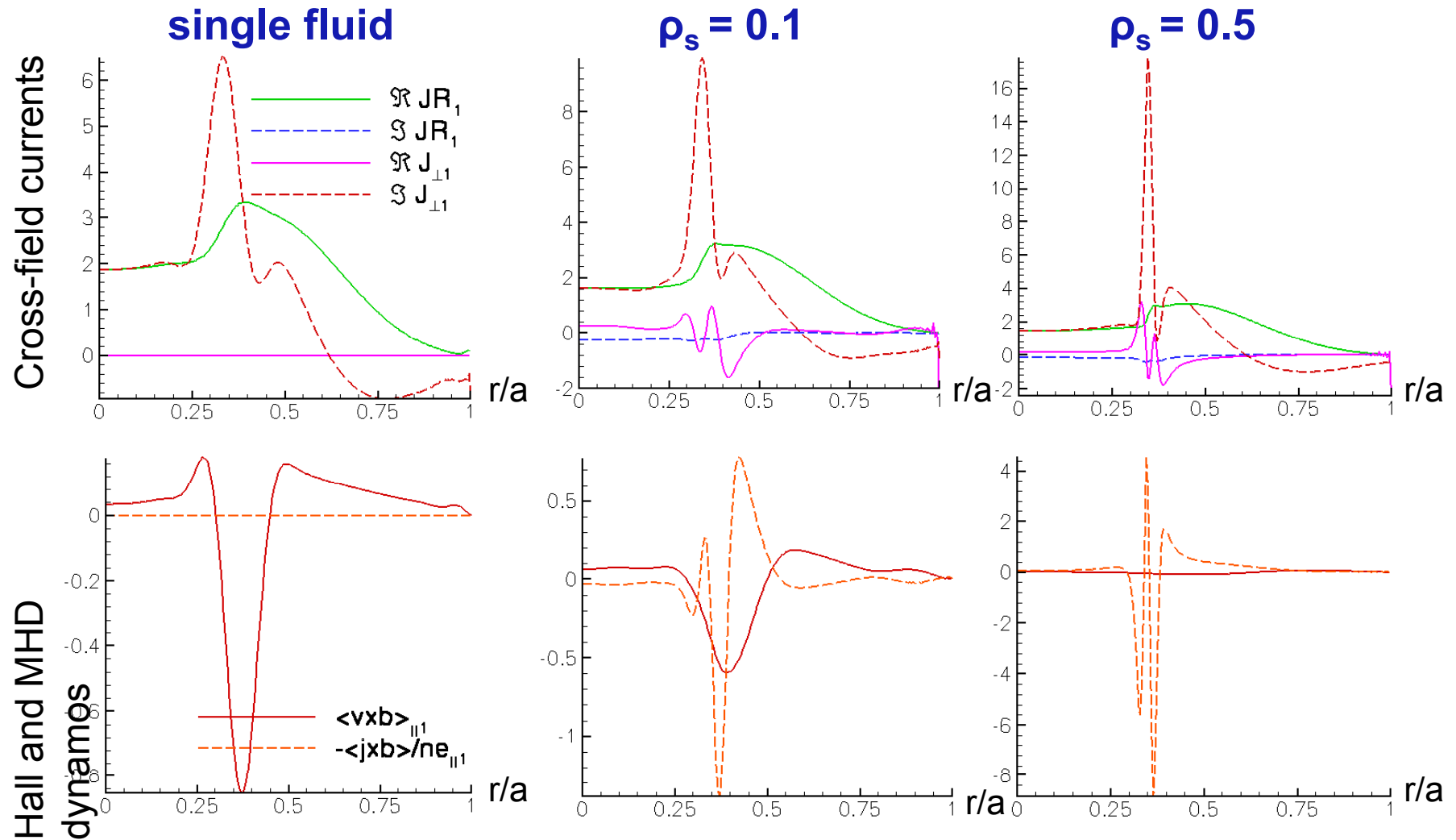
The amplitude of $\langle \mathbf{v}^{(1)} \times \mathbf{B}^{(1)} \rangle$ decreases in 2F case (consistent with the theory)



The magnitude of the quasilinear Hall dynamo varies with ρ_s and is localized at the rational surface



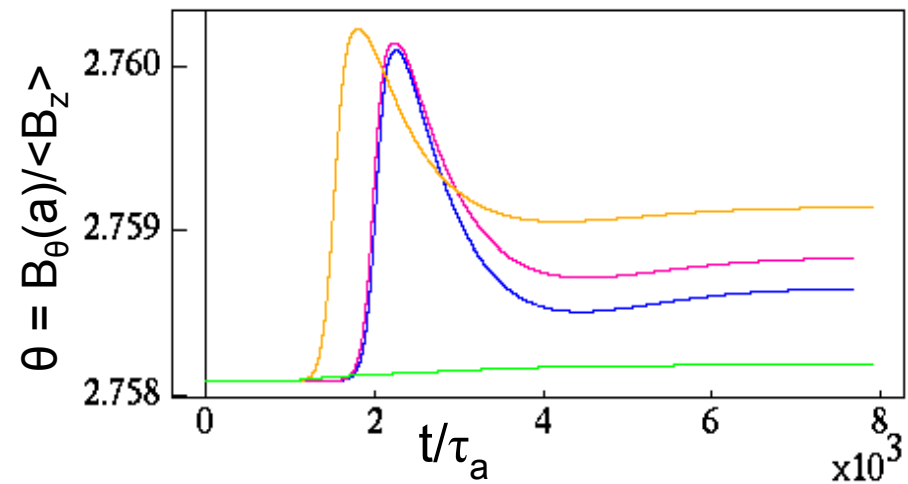
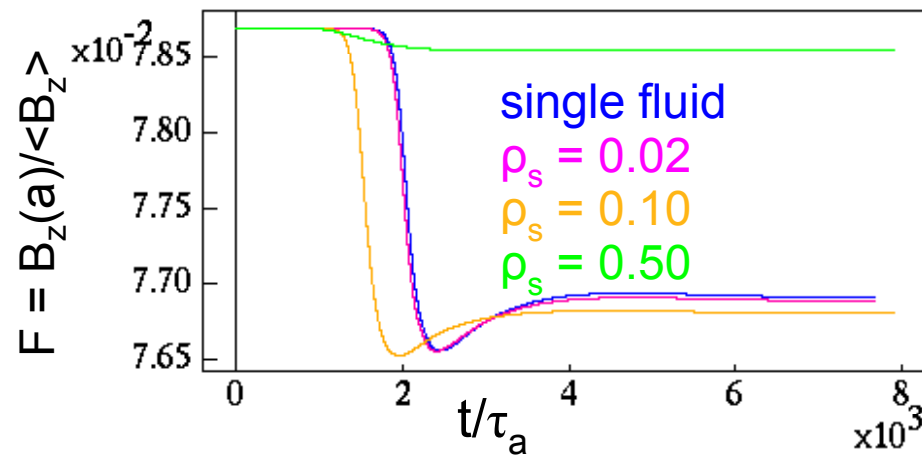
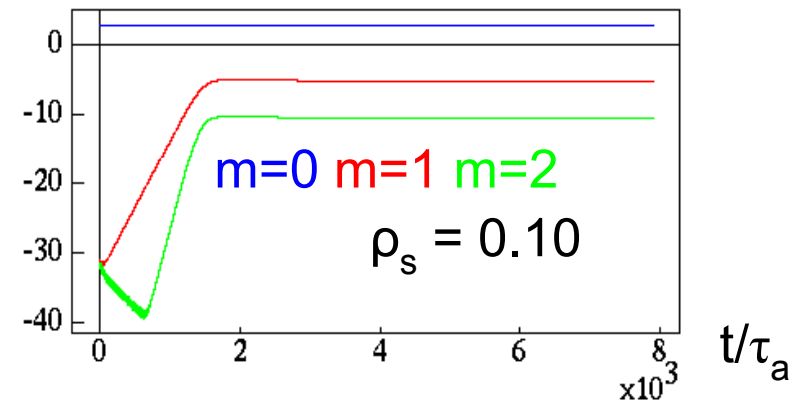
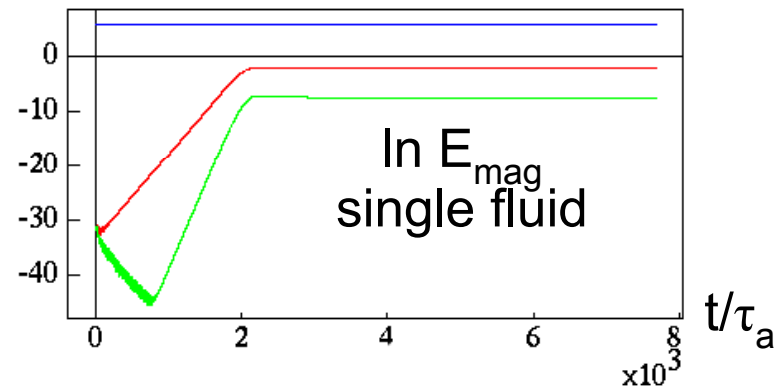
The Hall dynamo is determined by $\text{Re } J_{\perp}$, which is zero in the single fluid limit



Mean field modification takes place after the mode saturation



- small equilibrium field reconstruction is enough for nonlinear mode saturation

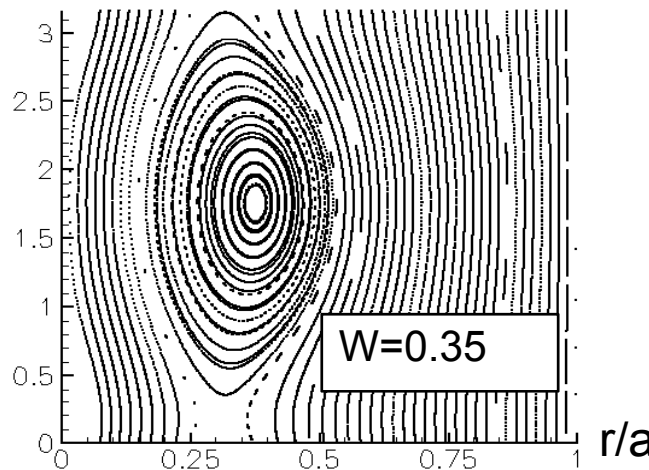
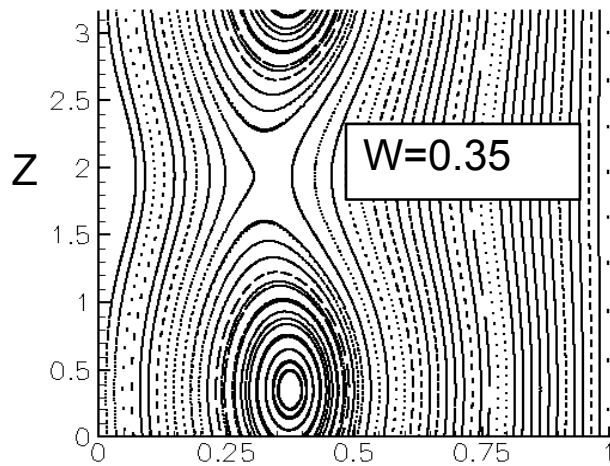
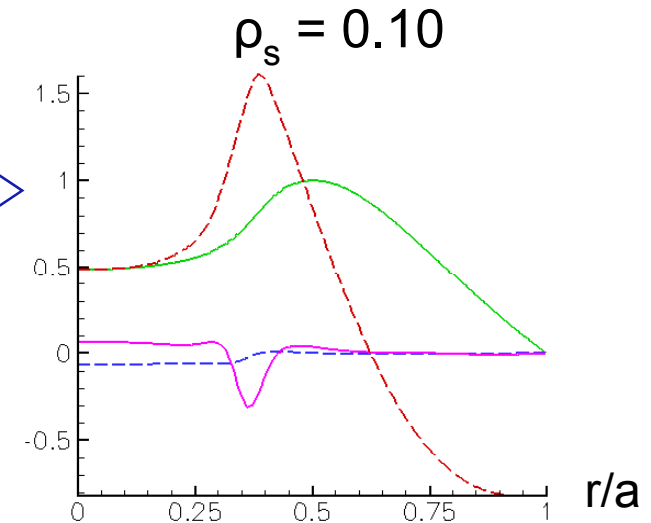
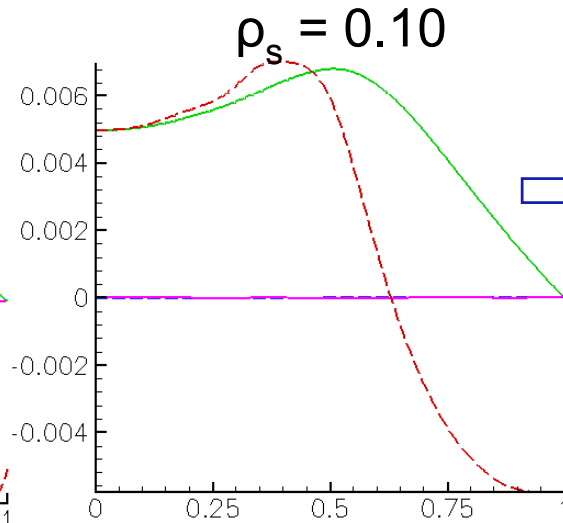
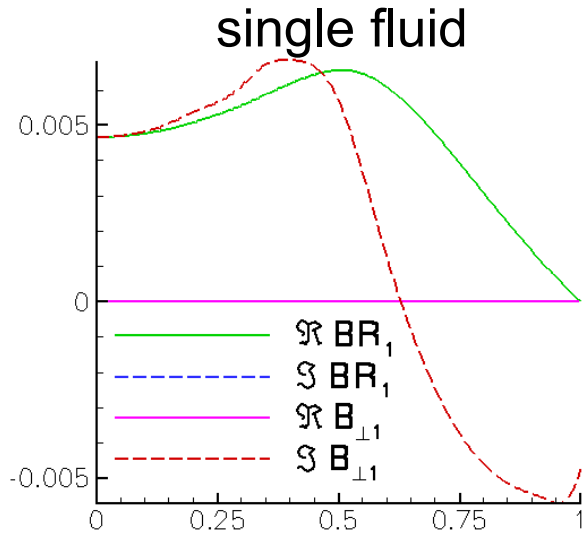


The saturated magnetic island is wider than the resistive layer



nonlinear saturation

linear stage



- unlike the linear cases, the out-of-phase nonlinear solutions are small
- island width is consistent with the theory

$$w = 4r_s \sqrt{\frac{B_r}{mB_\theta} \left(\frac{q}{rq'} \right)}$$

Both Hall and MHD dynamos are small in saturated state



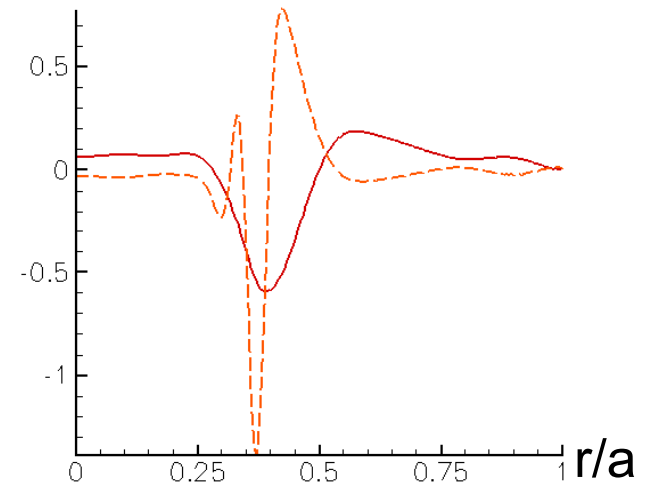
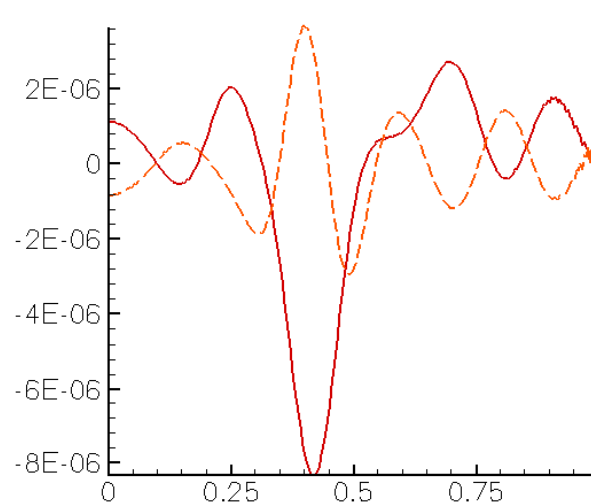
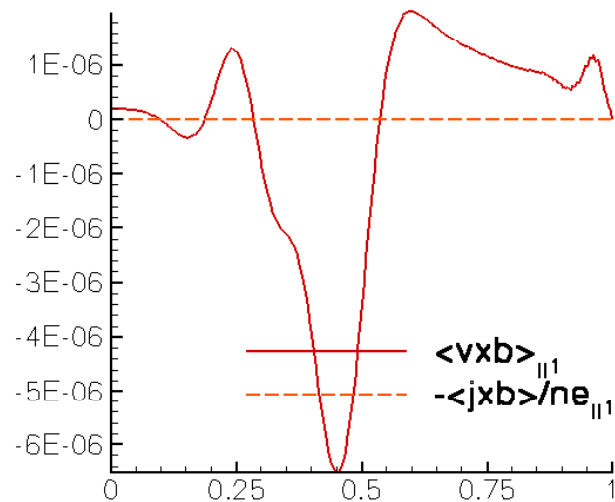
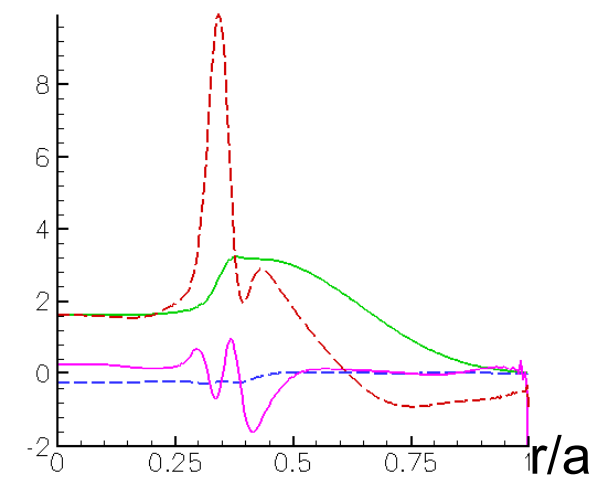
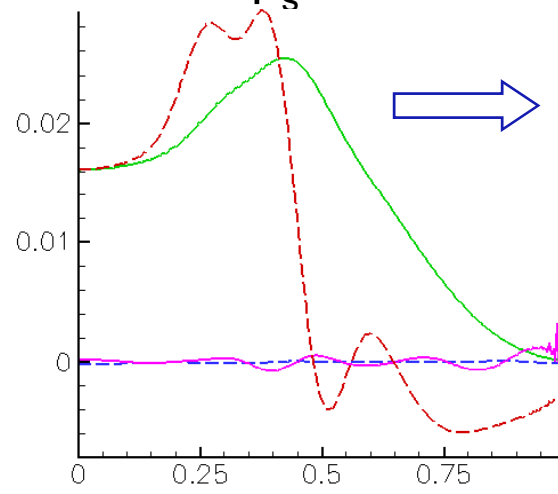
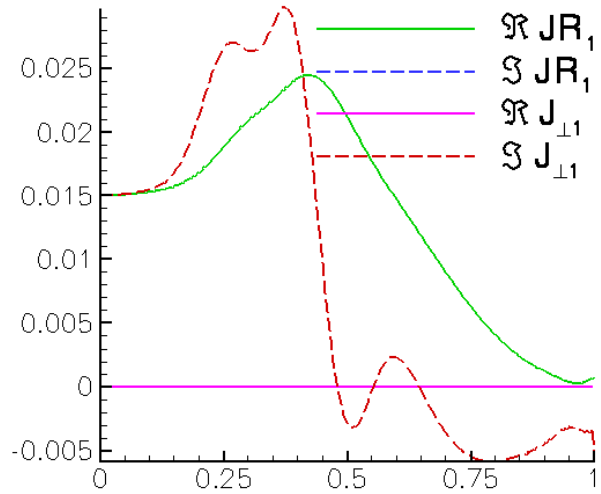
nonlinear saturation

linear stage

single fluid

$\rho_s = 0.10$

$\rho_s = 0.10$

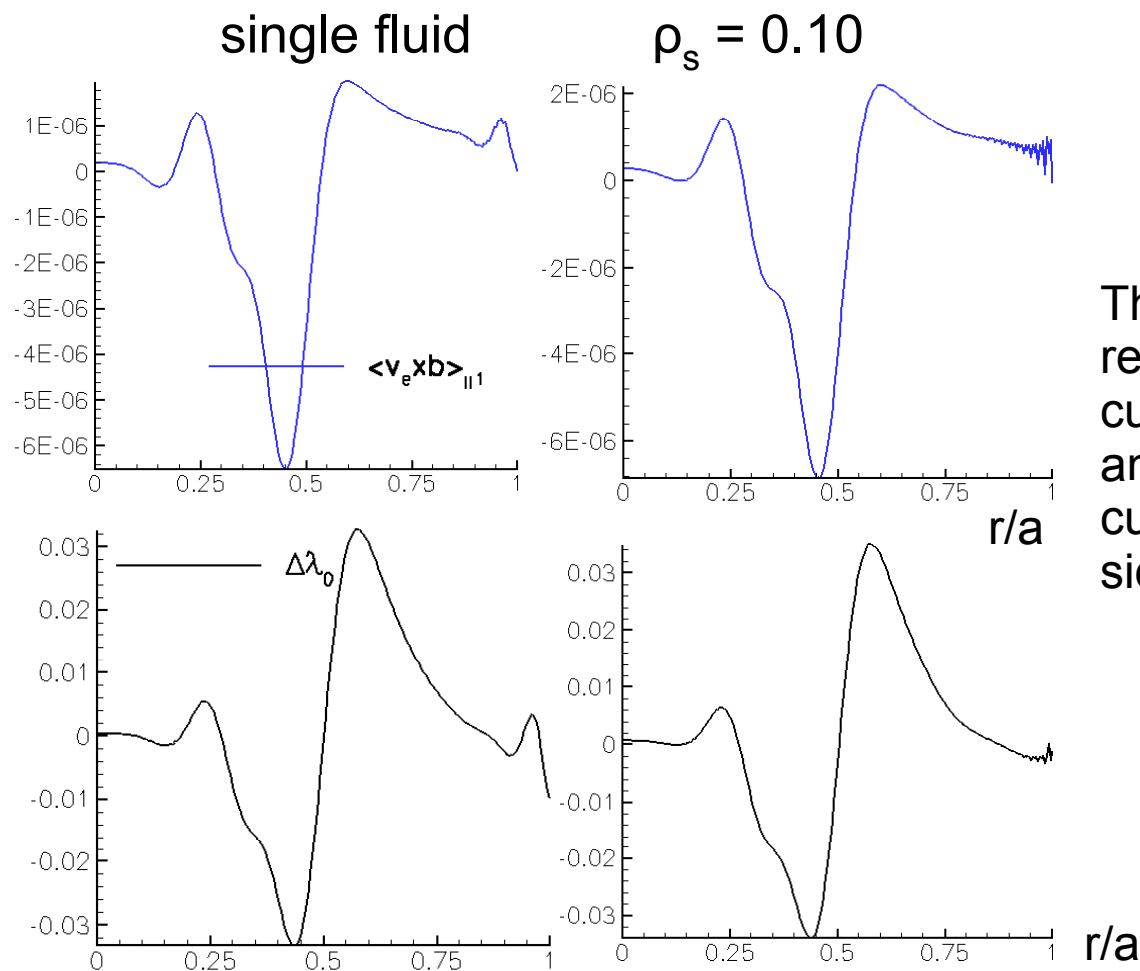


The overall shape of the parallel current modification is not sensitive to ρ_s



- Small modification of the equilibrium current $\Delta\lambda \sim 1\%$ is needed for saturation

$$\epsilon = \frac{1}{c} \langle \mathbf{v} \times \mathbf{B} \rangle_{\parallel} - \frac{1}{enc} \langle \mathbf{j} \times \mathbf{B} \rangle_{\parallel} = \frac{1}{c} \langle \mathbf{v}_e \times \mathbf{B} \rangle_{\parallel}$$

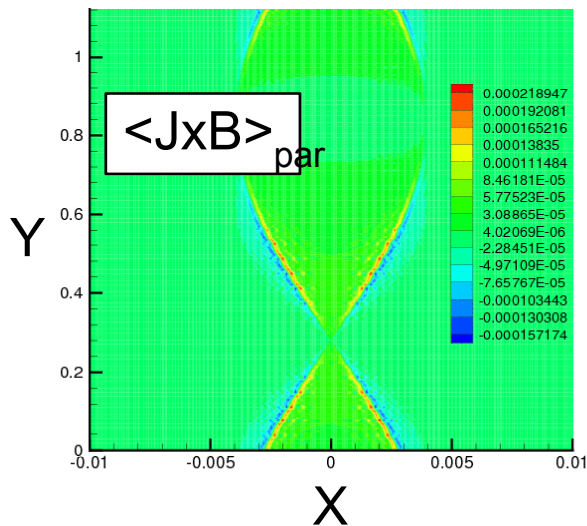
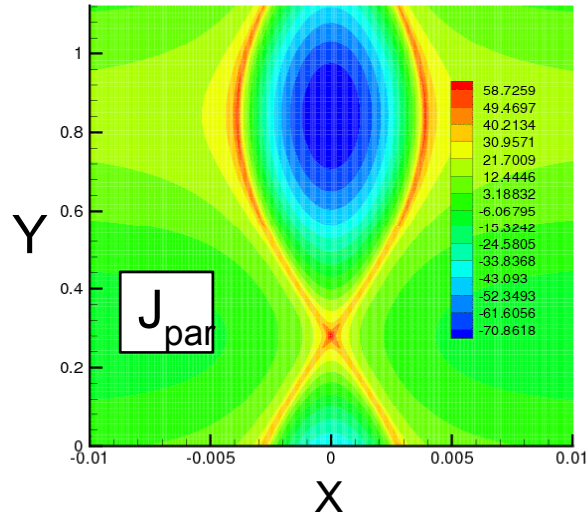


The saturated island reduces the parallel current inside the island, and enhances the parallel current on the outboard side of the island.

Fine structure of the slab model is not seen in cylindrical geometry

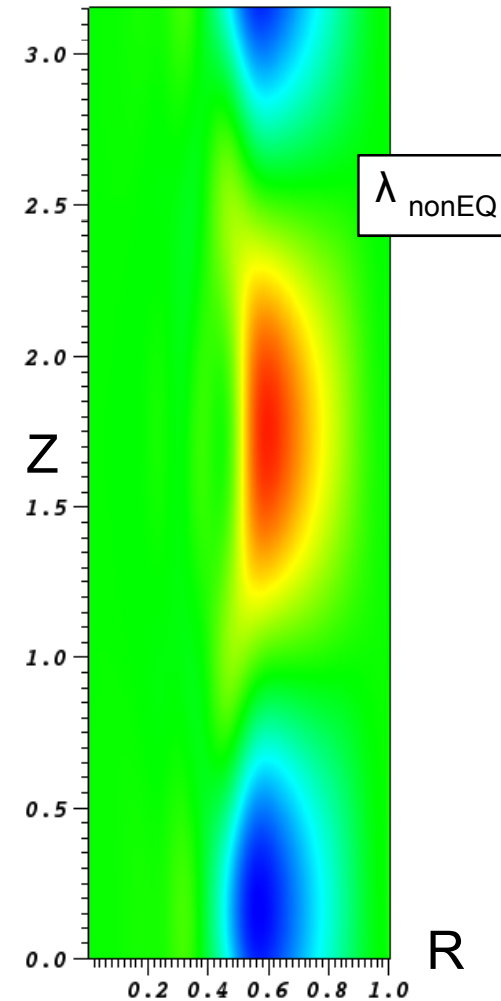


Slab Geometry



A characteristic of the fine structure is large $m, n \gg 1$ harmonics – this is not seen in the current calculations – the $m=2$ mode is small.

Cylindrical geometry



Summary



- Electron-ion decoupling on short scales affects the phases of the eigenfunctions creating a Hall dynamo absent in single fluid MHD.
- Two fluid effects and field line curvature cause a mode rotation even without diamagnetic flows.
- Quasilinear analytic predictions are confirmed by NIMROD simulations.
- **Small modification of the mean current is enough for the nonlinear mode saturation.**
- The magnitude of the saturated dynamo is small.
- **In saturated state, the radial profile of the total (MHD + Hall) dynamo is much less sensitive to ρ_s than during the linear stage.**
- Fine structure of the reconnection layer observed in slab simulations is not seen in the cylindrical case.